JOURNAL OF THE ROYAL SOCIETY Interface

The effect of population structure on the emergence of drug resistance during influenza pandemics

Florence Débarre, Sebastian Bonhoeffer and Roland R Regoes

J. R. Soc. Interface 2007 **4**, 893-906
doi: 10.1098/rsif.2007.1126

JOURNAL OF THE ROYAL SOCIETY Interface

J. R. Soc. Interface (2007) **4**, 893–906
doi:10.1098/rsif.2007.1126
Published online 3 July 2007

The effect of population structure on the emergence of drug resistance during influenza pandemics

Florence Débarre, Sebastian Bonhoeffer and Roland R. Regoes*

Institute of Integrative Biology, ETH Zürich, ETH Zentrum CHN, 8092 Zürich, Switzerland

The spread of H5N1 avian influenza and the recent high numbers of confirmed human cases have raised international concern about the possibility of a new pandemic. Therefore, antiviral drugs are now being stockpiled to be used as a first line of defence. The large-scale use of antivirals will however exert a strong selection pressure on the virus, and may lead to the emergence of drug-resistant strains. A few mathematical models have been developed to assess the emergence of drug resistance during influenza pandemics. These models, however, neglected the spatial structure of large populations and the stochasticity of epidemic and demographic processes. To assess the impact of population structure and stochasticity, we modify and extend a previous model of influenza epidemics into a metapopulation model which takes into account the division of large populations into smaller units, and develop deterministic and stochastic versions of the model. We find that the dynamics in a fragmented population is less explosive, and, as a result, prophylaxis will prevent more infections and lead to fewer resistant cases in both the deterministic and stochastic model. While in the deterministic model the final level of resistance during treatment is not affected by fragmentation, in the stochastic model it is. Our results enable us to qualitatively extrapolate the prediction of deterministic, homogeneous-mixing models to more realistic scenarios.

Keywords: influenza; metapopulation; drug resistance

1. INTRODUCTION

Recent human cases of H5N1 avian influenza have raised public concern. It is now considered an established fact that another influenza pandemic will occur sooner or later (e.g. Webby & Webster 2003). Given that our world is highly interconnected and interdependent (Hufnagel *et al.* 2004), this pandemic will certainly spread fast and widely.

Two types of antiviral drugs currently exist: the M2-inhibitors (M2I) and the neuraminidase inhibitors (NAI). M2Is target the M2 protein, an ion channel enabling the uncoating of the virion within the cell, which is a key step of the replication process. M2Is are only effective against influenza A (Stiver 2003). NAIs belong to a new class of antivirals including oseltamivir (*Tamiflu*), and zanamivir (*Relenza*). These drugs target the neuraminidase, which is required to release the budding virus from the cell and to prevent viral particles from clumping. NAIs therefore attenuate the infection.

A consequence of the use of antiviral drugs, however, is the emergence of drug resistance. Drug resistance in general is an urgent public health problem, costing human lives and money (Heymann 2006). Resistance against M2Is has risen rapidly over the past few years (Bright *et al.* 2006). The increasing incidence of M2I-resistant influenza A seems to be due to a high de novo resistance rate associated with low transmission fitness costs (Regoes & Bonhoeffer 2006). Given the chemical structure of oseltamivir, structural studies predicted some time ago that resistance to the drug could develop, allowing the NA to maintain its function (Moscona 2005). Several clinical cases have recently confirmed this prediction (de Jong *et al.* 2005). More alarmingly, transmission studies in ferrets and *in vitro* show that oseltamivir-resistant virus variants may differ in fitness and transmissibility. The $R292K$ mutation, which also shows cross-resistance to zanamivir, hampers growth and transmission of the virus, because it reduces the sialidase activity. Viruses carrying the $E119V$ mutation, however, have growth and transmission rates similar to wild-type viruses (Yen *et al.* 2005). In addition, it cannot be ruled out that a compensatory mutation could restore the fitness of other drug-resistant viruses.

These recent findings, combined with the fact that NAI drugs are being stockpiled world-wide underline the need for *in vivo*, *in vitro* and *in silico* studies to assess the emergence and spread of drug-resistant influenza viruses, under different public health interventions and patterns of drug use. In particular, computer simulations can provide guidelines for the

*Author for correspondence (roland.regoes@env.ethz.ch).

One contribution of 20 to a Theme Issue 'Cross-scale influences on epidemiological dynamics: from genes to ecosystems'.

Received 23 March 2007
Accepted 6 June 2007

most effective use of antiviral drugs (Stilianakis *et al.* 1998; Smith 2003), in terms of limiting both new infections and the emergence of drug resistance.

Recently, many complex models have been developed, that investigate the outcome of different public health interventions for controlling an influenza pandemic at the source (Ferguson *et al.* 2005; Longini *et al.* 2005), or for mitigating it once it has started to spread (Ferguson *et al.* 2006; Germann *et al.* 2006). These interventions include treatment and prophylaxis with antiviral drugs, vaccination, quarantine, restrictions on travel, school closure and other non-pharmaceutical interventions. Although these studies often mention the risk of the emergence and spread of drug-resistant viruses, none of them explicitly investigates the dynamics of resistance emergence. Some models, however, have already assessed the potential spread of drug-resistant viruses for M2Is (Stilianakis *et al.* 1998) as well as oseltamivir (Ferguson *et al.* 2003; Regoes & Bonhoeffer 2006). None of these studies took into account the spatial population structure, although Ferguson *et al.* (2003) incorporated population structure in terms of risk groups and age structure.

In this paper, we investigate the emergence and spread of oseltamivir-resistant influenza virus in a population structured into subpopulations (metapopulation), when different public-health interventions are performed. The work extends the studies of Stilianakis *et al.* (1998) and Regoes & Bonhoeffer (2006). First, we modify the initial model, and then extend it to a metapopulation. Then, we develop a stochastic version of the model. We implement spatial structure in a very abstract and generic way, rather than attempting to mimic the real world situation. This allows us to qualitatively investigate how spatial structure influences the epidemic and the efficacy of interventions.

2. MODELS AND METHODS

We extended a previously published model describing an influenza outbreak in a school (Stilianakis *et al.* 1998) into a metapopulation model, i.e. we linked multiple epidemic foci by allowing individuals to migrate between them. We developed deterministic and stochastic versions of this metapopulation model.

2.1. Structure of the community

Different metapopulation structures can be studied in epidemiology, depending on what is defined as a patch (Hess *et al.* 2002). Given the organization of humans in well-defined spatial structures such as families, villages and towns (Grenfell & Harwood 1997), patches are groups of hosts in our model. Colonization of a patch corresponds to the establishment of an infection in a patch harbouring susceptible individuals. Local extinction of the disease occurs when all the infected hosts within the patch are removed (through recovery or death). It is also assumed that there is a homogeneous mixing within each subpopulation (figure 1).

We connect the disease dynamics within the patches by allowing individuals to migrate from one patch to the other. Mathematically, the migration process of

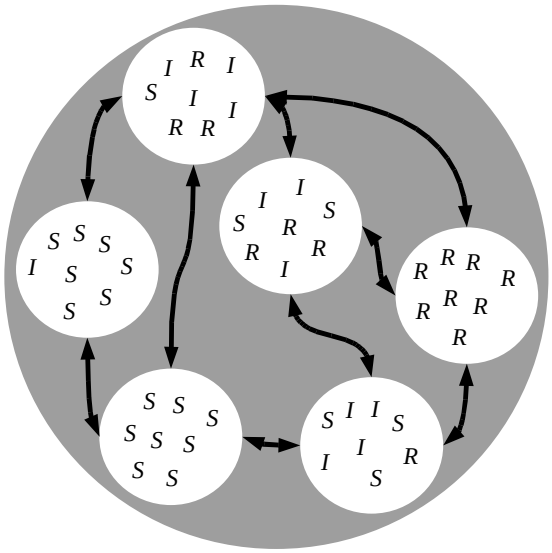

Figure 1. Structure of the population. The grey circle represents the whole population, white circles represent patches, arrows represent migration of individuals between patches. *S*, *I* and *R* stand for susceptible, infected and removed, respectively. The bottom-left patch is still disease-free, while the patch on the left has just been colonized. The parasite is locally extinct in the patch on the right.

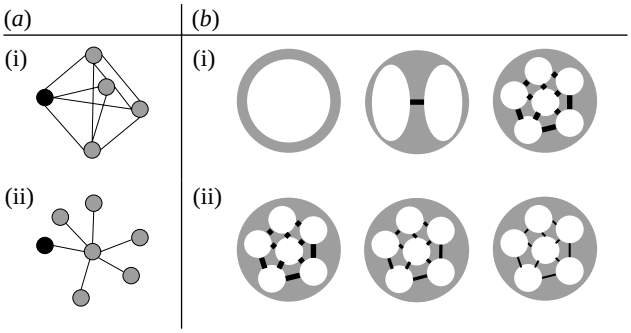

Figure 2. Population structures. (*a*) Different types of connections among subpopulations: (i) island and (ii) spider (these names were used by Hess (1996)). The black node is the one where the infection starts. (*b*) From the left to the right, increasing heterogeneity of mixing: (i) the number of subpopulations increases and (ii) the migration coefficient decreases. Throughout the paper, we assume that the total population size is $N=500$.

individuals between patches is described as migration matrix $M=(\mu_{i,j})_{\substack{1<i<n,\\1\leq j\leq n}}$, where μ_{ij} is the rate of migration of individuals from population i to population j. This matrix determines the topology and the strength of the connections between the patches.

We model different population structures. Throughout this paper, the term *population structure* refers to the number of subpopulations, and to how they are connected (i.e. which subpopulations are connected, and what is the value of the migration rate). For a given number n of subpopulations, two types of subpopulation connections are investigated here (figure 2*a*). In the *island*-type of connections, all the subpopulations are interconnected; in the *spider*-type, $n-1$ subpopulations are connected only to a central one, and the infection starts in a peripheral subpopulation. For a given

structure, a range of migration coefficients (the nonzero coefficients in the migration matrix) and of number of subpopulations (the size of the matrix) are investigated (figure 2*b*). We assume that migration is the same among connected subpopulations, which means that

$$\forall (i,j) \in \{1,\ldots,n\}^2,$$

$$\mu_{i,j} = \begin{cases} 0 & \text{if subpopulations } i \text{ and } j \text{ are not connected} \\ m & \text{otherwise} \end{cases},$$

and that all subpopulations have the same size N/n, where N is the total number of individuals and n the number of subpopulations. We chose a population size of $N=500$ because larger population sizes would have rendered simulations too long to run. A population of 500 individuals might not seem realistic for an influenza pandemic. We made sure, however, that the size of the population had no impact on our conclusions. (See appendix C2 for simulations with a bigger population size.)

There is no age or social structure in the population and no seasonal variation of parameters (because we focus on the first 100 days of the epidemic only).

2.2. Epidemic parameters

The parameters of the model are listed in appendix A and were chosen to match with recent studies on oseltamivir-resistant viruses (Gubareva *et al.* 2001; Kiso *et al.* 2004).

R_0, the basic reproductive number, is a key concept in epidemiology (Heffernan *et al.* 2005). It is defined as the number of secondary cases produced by a single infected individual during its entire infectious period, in a fully susceptible population (Diekmann *et al.* 1990; Anderson & May 1991). The transmission rates (the βs) are scaled so that the basic reproductive number of the sensitive strain, R_0^{s}, is equal to 4.5 without drugs, and R_0^{r}, the basic reproductive number of the resistant strain, equals 0.45. The next generation method (Diekmann *et al.* 1990; Heffernan *et al.* 2005), which is described in appendix B, was used to determine the R_0^{s} under different interventions (table 1).

Our R_0^{s} is high when compared with the range used in recent models (always lower than 2.5 in Ferguson *et al.* (2005, 2006), Longini *et al.* (2005), Germann *et al.* (2006)). However, our value was estimated by Stilianakis *et al.* (1998) from data collected during an outbreak in a boarding school. It may be higher because a boarding school population is more homogeneously mixed than that of an entire town. If one estimated R_0^{s} on the basis of data generated by our model (with $R_0^{\mathrm{s}} = 4.5$) using a homogeneously mixed model (e.g. Mills *et al.* 2004), the estimate of R_0^{s} would be lower than 4.5 because the disease spreads slower in our model than in a homogeneous-mixing model. Hence, our choice of $R_0^{\mathrm{s}} = 4.5$ is not inconsistent with epidemiological data.

For R_0^{r} we assumed a 10-fold resistance cost. Given the fact that oseltamivir-resistant strains found in humans to date are not transmissible (Herlocher *et al.* 2002, 2004), our R_0^{r} may appear too high. However, because the large-scale use of oseltamivir may soon select for transmissible resistance, and compensatory mutations may reduce potential costs even further, one may argue that our R_0^{r} is too low to describe oseltamivir-resistant influenza strains that may emerge during a future pandemic. With our choice of R_0^{r} we try to strike a compromise between these two opposing views. Our results, however, seem to be robust with regard to the value of R_0^{r} (see simulations performed with higher values of R_0^{r} in appendix C1).

Table 1. R_0 values of the sensitive (s) and resistant (r) viruses for different interventions.

	no drugs	treatment	prophylaxis
R_0^{s}	4.5	2.6	0.2
R_0^{r}	ϕ	0.45	0.45

2.3. Deterministic model

Although containing many more classes, the model that we use to study the emergence of resistance is based on the classical *SIR* model (Kermack & McKendrick 1927). The set of equations describing the epidemic without any public health intervention corresponds to an $SII_{\mathrm{s}}R$ model. Infected people are divided into asymptomatic (I) and symptomatic (I_{s}) classes. Both of them are infectious, but their infectiousness varies, and only those who develop clinical symptoms will be treated, when treatment is provided. See appendix A for a complete description of the equations.

Two kinds of interventions will be considered.

— *Treatment*. All symptomatically infected individuals receive treatment (oseltamivir).

Infected people receiving treatment are less infective, develop symptoms more slowly and recover faster.

— *Prophylaxis*. In addition to treatment of all symptomatic individuals, uninfected as well as asymptomatically infected individuals (as they appear to be uninfected) receive prophylaxis (oseltamivir).

Prophylaxed susceptibles become less susceptible to infection, while asymptomatically infected people are less infectious and recover faster.

While treatment is a continuous intervention, prophylaxis is not. At a given time, all the susceptible and asymptomatically infected individuals receive prophylaxis, and are then moved to the corresponding treated class.

Neither treatment nor prophylaxis has any effect on people infected by a resistant virus. Note that throughout the paper, a *resistant virus* refers to a drug-resistant virus, and that a *resistant case* refers to an individual shedding drug-resistant viruses.

More classes are required when interventions are performed, in order to represent individuals receiving treatment or prophylaxis.

— Infected individuals are distinguished according to whether they are symptomatically infected (s) or

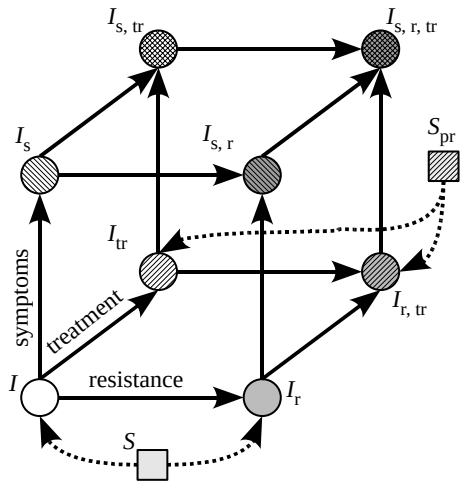

Figure 3. Schematic of the model. The eight different infected classes can be represented on a cube. The axes are resistance, treatment, symptoms. New infected individuals enter the cube from its bottom (i.e. no symptoms) side, because symptoms do not appear immediately after infection. On this side, the new infected individuals go to the 'resistant' edge (i.e. the $I_r - I_{r,tr}$ edge) if they have been infected by an individual shedding resistant viruses (i.e. by an I_r, $I_{s,r}$, $I_{r,tr}$, or $I_{s,r,tr}$), and they go to the 'treated' edge (i.e. the $I_{tr} - I_{r,tr}$ edge) if they had received prophylaxis (i.e. if they were S_{pr}).

not, treated (tr) or not, and have developed resistance (r) or not (figure 3).
— Susceptible individuals can receive prophylaxis (pr) or not.

For each class C, $C \in \{S, S_{pr}, I, \ldots, I_{s,r,tr}\}$, C_i refers to the number of individuals of this class present in subpopulation i, $1 \leq i \leq n$. Moreover, migration terms are added to the equations described in Regoes & Bonhoeffer (2006). For C_i, this migration parameter is of the following form:

$$\mathcal{M}(C_i) = -\sum_{j=1}^{n} \mu_{i,j} \cdot C_i + \sum_{j=1}^{n} \mu_{j,i} \cdot C_j. \qquad (2.1)$$

The first term refers to individuals of class C leaving subpopulation i for subpopulation j, while the second term refers to individuals arriving (see appendix A3 for the whole equations).

The ODEs were solved numerically using R's odesolve package (R Development Core Team 2005; Setzer 2005). We also determined how many people are infected during an epidemic (i.e. 'total number of infected cases'), among them, how many shed resistant viruses (i.e. 'total number of resistant cases'), and among the latter, what is the proportion of resistance that appeared de novo (i.e. appeared during infection, as opposed to transmitted resistance). See appendix A3 for formulae.

2.4. Stochastic model

The deterministic version of the model is made stochastic by using an implementation of the Gillespie algorithm (Gillespie 1976), which numerically simulates a Markov process. The Gillespie algorithm was coded in R for the purpose of this study. For each set of parameters, at least 100 stochastic simulations are run using this algorithm.

Since computing time increases exponentially with the division of the population (i.e. the number of subpopulations, or the number of different equations), simulations were run on a cluster of computers. Parallelization was performed *by hand*, by submitting different jobs corresponding to different sets of parameters to individual nodes of the computer cluster.

3. RESULTS

3.1. Deterministic model

In this section, we investigate the impact of population structure and of different interventions on the dynamics and the final outcome of the epidemics, focusing on the development of drug resistance. The deterministic version of the model is used here.

3.1.1. Dynamics and final outcome of the epidemics after treatment. How does the structure of the population affect the dynamics of the epidemic as compared with a homogeneously mixed model? To answer this question, and for the sake of simplicity, we use the epidemic's peak time and value (i.e. the maximal instantaneous number of infected individuals in the whole population) to characterize the dynamics of the epidemic.

Figure 4 shows dynamical and final features of the epidemic for different population structures. For a larger population of 5000 individuals, figure 4 does not change. This is due to rescaling of the transmission rates such that the basic reproductive number remains the same (equation A 9). Figure 4*a*,*b*,*d*,*e* shows that the epidemic peak decreases and occurs later with decreasing migration rates. This means that the epidemic is less explosive in a fragmented population than in a homogeneous population. Treatment slows down the epidemics and reduces its peak. As expected, the level and the timing of the peak converge to the homogeneous mixing case for high migration rates.

Some results in figure 4 might appear counter-intuitive: the peak time and value with 15 subpopulations (crosses) are between the values for 1 (circles) and 5 (triangles) subpopulations. As discussed later in §3, when the population is subdivided into more than one subpopulation connected according to the island model, there are two peaks, corresponding to epidemics in the focal subpopulation (first peak) and later in the peripheral subpopulations (second peak). The second peak in a model with a fragmented population is generally smaller than the only peak in a model with a homogeneous population because the total number of susceptible individuals in the peripheral subpopulations is smaller than that of the total population. This explains why the peak value in the non-fragmented population is highest. With increased numbers of subpopulations, however, the total number of susceptible individuals in the peripheral subpopulations increases. That is why the peak value is higher for 15 subpopulations than for 5 (figure 4*b*,*e*).

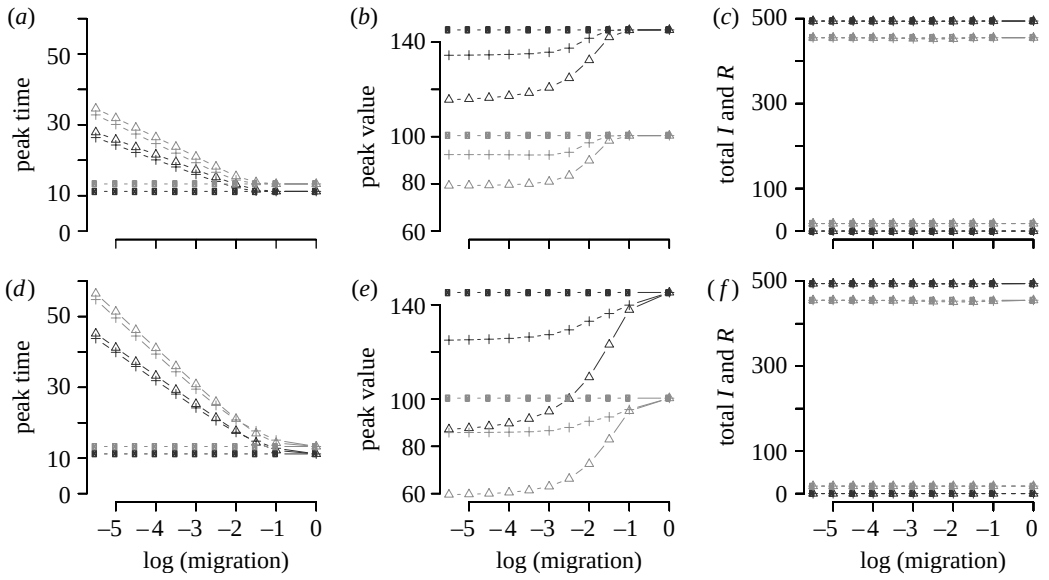

Figure 4. Impact of population structure and of public health interventions on the dynamics and final outcome of the epidemic. Structures: island (*a–c*), spider (*d–f*); interventions: no drugs (dark grey), treatment (grey); number of subpopulations: 1 (circle), 5 (triangle) and 15 (cross). The total size of the populations is $N=500$. (*a*) Time of the epidemic's peak as a function of migration, in days. (*b*) Value of this peak. (*c*) The total number of infected and resistant cases. Note that the results of the prophylaxis intervention are not shown here because they depend strongly on the number of subpopulations and the migration coefficient.

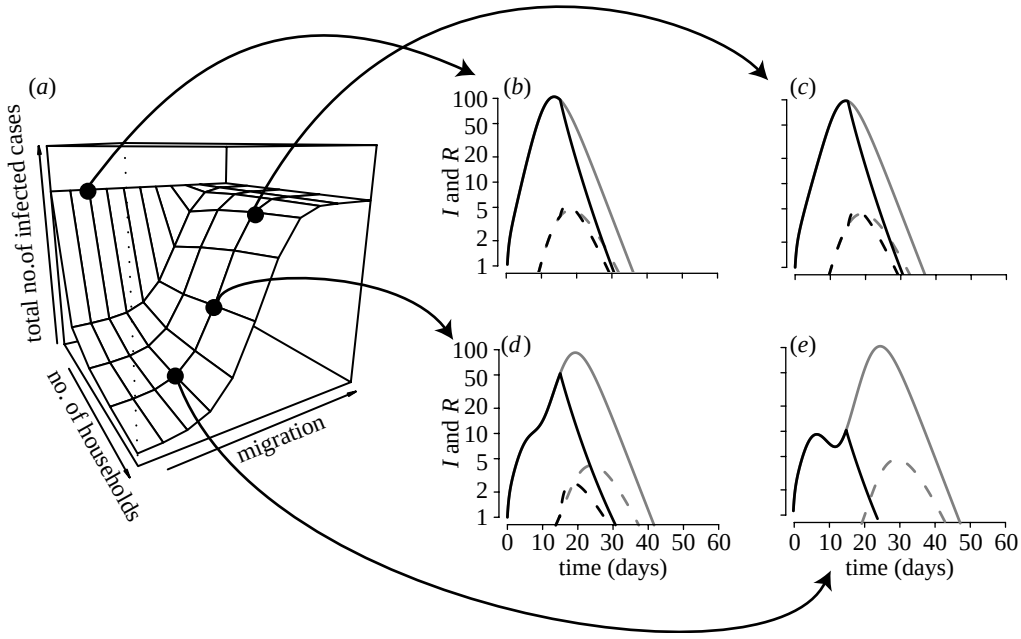

Figure 5. (*a*) The total number of infected cases as a function of the structure of the population. (*b–e*) Time course for selected points. The population is island-shaped, its total size being $N=500$ individuals, and prophylaxis starts on day 15. (*b*) A homogeneous population. (*c–e*) Fifteen subpopulations. The migration coefficient is 10^{-2}, 10^{-3} and 10^{-4} in (*c*), (*d*) and (*e*), respectively. (*b–e*) The population mixes less and less homogeneously. Grey, treatment; black, prophylaxis. Solid line, infected cases; dashed line, resistant cases.

The results with regard to the time of the peak can be explained as follows: in a single subpopulation, the speed of the epidemic decreases with its size. Hence, if the population is more fragmented the epidemics spread faster in each subpopulation. This accounts for the result concerning the peak time (figure 4*a*,*d*).

The fragmentation of the population, however, has no impact on the final outcome of the epidemic, in terms of the total number of infected and resistant cases (figure 4*c*,*f*). This is due to the fact that the total numbers of infected (I) and resistant (R) cases solely depend on the basic reproductive number, R_0, of each strain, which is independent of the migration rate. Without drugs almost everyone (98.8%) gets infected. Treatment slightly decreases this value to 91%. Nevertheless, treatment also allows the emergence of resistant cases, which represent 3.8% of the infected cases.

These results raise the following questions: can prophylaxis more efficiently decrease the total number

of infected cases? Does it lead to more resistance than treatment? And lastly, when should prophylaxis be performed?

3.1.2. Prophylaxis: the impact of timing. The total number of infected and resistant cases during the epidemic is lower when prophylaxis is performed (figure 5). The results are similar with a bigger population size. Unlike with treatment, the outcome of prophylaxis depends on the structure of the population. The higher the degree of fragmentation of the host population is, the fewer is the number of people getting infected during the epidemic (figure 5*a*). For instance, with our parameters, and with proph.start = 15 (where proph.start denotes the time at which prophylaxis is initiated), 80% of the population finally gets infected during the epidemic in a homogeneously mixing population, while only 5% gets infected when the number of subpopulations is high or the migration is low. In both cases, around 4% of infected people shed resistant viruses. This is due to the shape of the epidemic curve: the higher the degree of fragmentation, the more peaks there are. Note that there are at most two peaks with an island shape: the first peak corresponds to the focal subpopulation, where the epidemic starts, and the second peak to all the other subpopulations, which are directly linked to the focal one. Note also that if the mean distance to the focal subpopulation is greater than 1 (e.g. with the spider shape, data not shown), there are more than two peaks. The state of the epidemic at which it is 'hit' by prophylaxis (peak or trough, figure 5*b–e*) depends on the structure of the population. After prophylaxis is initiated both R_0^s and R_0^r become abruptly less than 1, and the epidemic wanes, because both resistant and sensitive variants cannot sustain the epidemic anymore.

Owing to the fact that the structure of the population influences at which state the epidemic is hit by prophylaxis, the timing of prophylaxis has an impact on resistance emergence (figure 6). The earlier the prophylaxis is initiated, the fewer are the infected and resistant cases during the epidemic and the greater the proportion of infected people shedding resistant viruses. The fact that $R_0^r > R_0^s$ when everybody receives drugs accounts for this higher proportion of resistance when proph.start is smaller. Even though unable to trigger a real epidemic, the resistant variant outcompetes the sensitive one. We also determined the proportion of transmitted resistance versus de novo resistance. This proportion is substantially higher when proph.start is small, again because sensitive variants are outcompeted earlier.

3.2. Stochastic model

3.2.1. The impact of population structure. Even in homogeneous populations, stochastic simulations differ from deterministic ones in some respects. First, around 40% of the simulations did not generate any secondary case (the first infected is an *I*, asymptomatic, non-treated, shedding sensitive viruses). Then, due to local extinctions, the stochastic model predicts fewer infected cases on average than the deterministic model (figures 7 and 8). Furthermore, the total number of

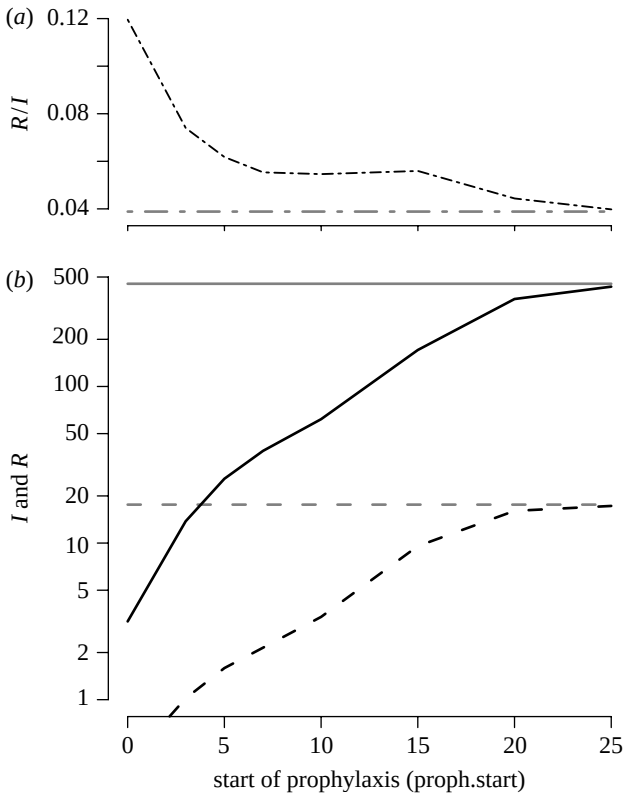

Figure 6. Impact of the timing of prophylaxis compared to treatment (*a*) on the proportion of resistance and (*b*) on the total number of infected and resistant cases. There are 10 subpopulations, the total size of the population being $N = 500$ individuals, and migration $= 10^{-3}$. Grey, treatment; black, prophylaxis. Solid line, infected cases; dashed line, resistant cases; dot-dashed line, proportion of resistant cases among the infected.

infected people during the epidemic is lower in the stochastic than in the deterministic model (e.g. approximately 80% of the population compared with 98.8% with the deterministic version).

Unlike the deterministic model, the structure of the population has an impact on the outcome of the epidemic even without drugs or under treatment (figure 9). The higher the degree of fragmentation of the host population, the less the infection spreads. When the number of subpopulations is high, or when migration between subpopulations is low, the epidemic is often restricted to a small number of subpopulations (most of the time to only the one where the epidemic started). Comparing the effect of different interventions, we find that treatment does not substantially reduce the total number of infected cases, but leads to the emergence of resistance (figure 9). On the other hand, as in the deterministic model, prophylaxis has a strong impact on the total number of resistant cases. We also find that the proportion of resistant cases among infected people is higher with prophylaxis (between 3 and 6% when proph.start = 10). This result is, as in the deterministic case, due to the change of the basic reproductive numbers when different interventions are performed.

3.2.2. Prophylaxis: impact of timing. In spite of the variance in the prediction due to stochasticity, the impact of prophylaxis timing is qualitatively the same

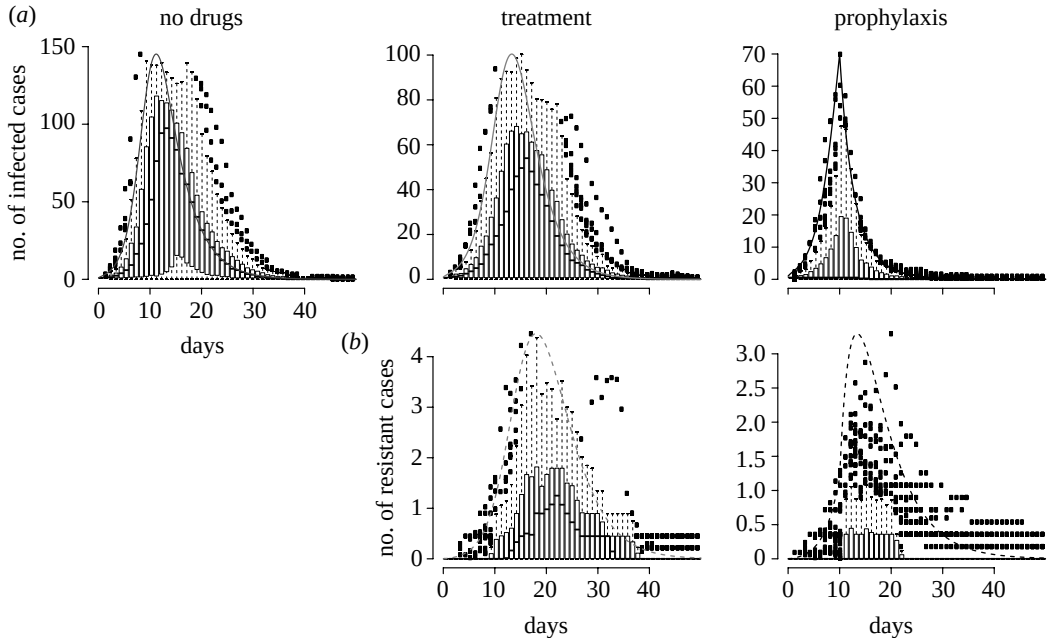

Figure 7. A comparison between deterministic and stochastic versions of the model without population structure. We assumed only one population of 500 individuals, and that prophylaxis starts on day 10. The smooth curve is the prediction of the deterministic model, and the box and whiskers plots summarize realizations of the stochastic model (we show here only the realizations in which there was at least one secondary case among the 100 runs). (*a*) Infected cases over time. (*b*) Resistant cases over time.

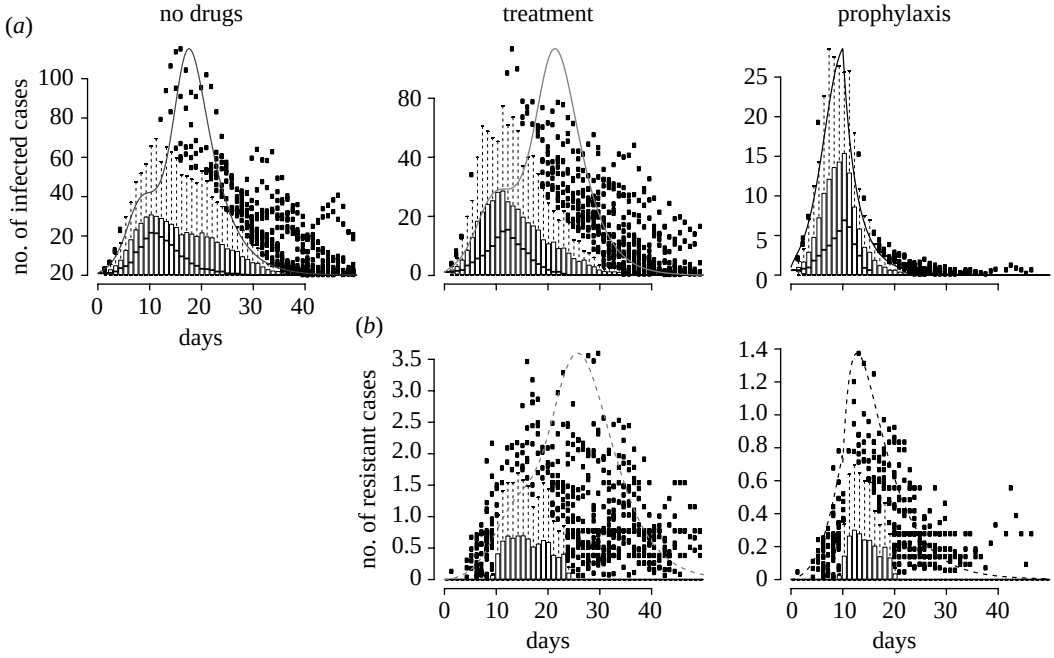

Figure 8. A comparison between deterministic and stochastic versions of the model with population structure. There are four subpopulations, the total size of the population being $N=500$, the migration rate is 10^{-3}, and prophylaxis starts on day 10. The smooth curve is the prediction of the deterministic model, and the box and whiskers plots summarize realizations of the stochastic model (again we show here only the realizations in which there was at least one secondary case among the 100 runs). (*a*) Infected cases over time. (*b*) Resistant cases over time. Note that with population structure the difference between stochastic and deterministic simulations is mainly due to the stochasticity of migration.

as in the deterministic model. The earlier prophylaxis starts, the smaller is the number of infected and resistant people during the epidemic (figure 10). For a larger population of $N=5000$ we obtain very similar results (see figure 13 in appendix A).

The result concerning the proportion of resistant cases is less clear in the stochastic model. Although, as in the deterministic model, the mean number of resistant cases is higher for prophylaxis starting early, the variance is also higher. In some simulations, the proportion of resistance is very low (for instance $R:I=0:10$ in one simulation), while it is very high in some others ($R:I=6:9$ in another). Moreover, among simulations that led to the emergence of resistance, the proportion of transmitted resistant strains decreases with the timing of prophylaxis: approximately 30% of

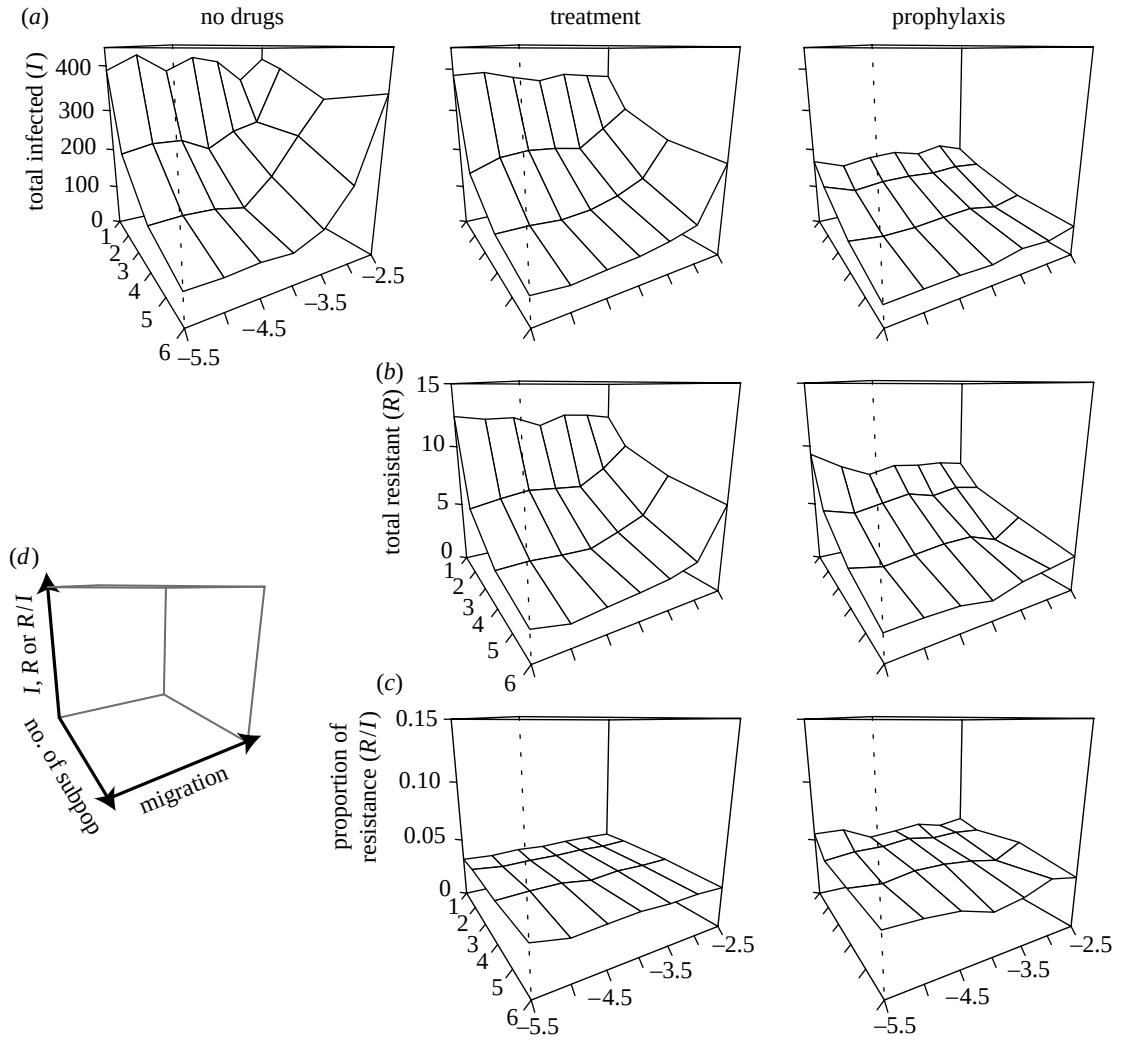

Figure 9. Impact of population structure on the total number of (*a*) infected and (*b*) resistant cases, and on (*c*) the proportion of resistance, for each of the three interventions. The total size of the population is $N=500$ and prophylaxis starts on day 10. The legends of the axes are on (*d*).

transmitted resistance when prophylaxis starts at day 0, approximately 20% at day 5, but less than 5% at day 20 (data not shown). Note that there is almost no transmitted resistance when treatment is performed. In brief, if resistance appears when prophylaxis starts early, resistant strains are more likely to be transmitted than if prophylaxis is initiated later.

4. DISCUSSION AND CONCLUSION

The planned, widespread use of NAI for treatment and prophylaxis during influenza pandemics is likely to lead to the emergence of drug-resistant influenza strains. In this study, we investigated the effect of population structure on the emergence of drug resistance during pandemics using mathematical models. To this end, we constructed deterministic and stochastic metapopulation models describing the spread of pandemic influenza strains.

We show that epidemic outbreaks in fragmented populations are less explosive. In a deterministic model, however, the fragmentation of the population has no influence on the final level of drug resistance in the population when nothing is done or when drugs are given to symptomatic individuals. In contrast, when antivirals are delivered prophylactically to non-symptomatic individuals in addition to treating symptomatic individuals, population structure and the timing of prophylaxis interact synergistically in resistance development and influence the proportion of resistance due to the transmission of resistant variants.

The results of the stochastic model are different in some respects. First, 40% of the epidemics go extinct very rapidly. Moreover, when the epidemic does not go extinct, the number of infected and resistant cases is still lower than in the deterministic model. This is due to an interaction of stochasticity and migration. In addition, the final level of resistance after treatment only is affected by the structure of the population, and not by stochasticity.

This study should be considered as a conceptual work, aiming to study qualitative trends, rather than to make quantitative predictions. Even though many of our model parameters are based on published studies on influenza (see Regoes & Bonhoeffer (2006) for a justification of the parameters), the topological features and parameters describing the structure of the

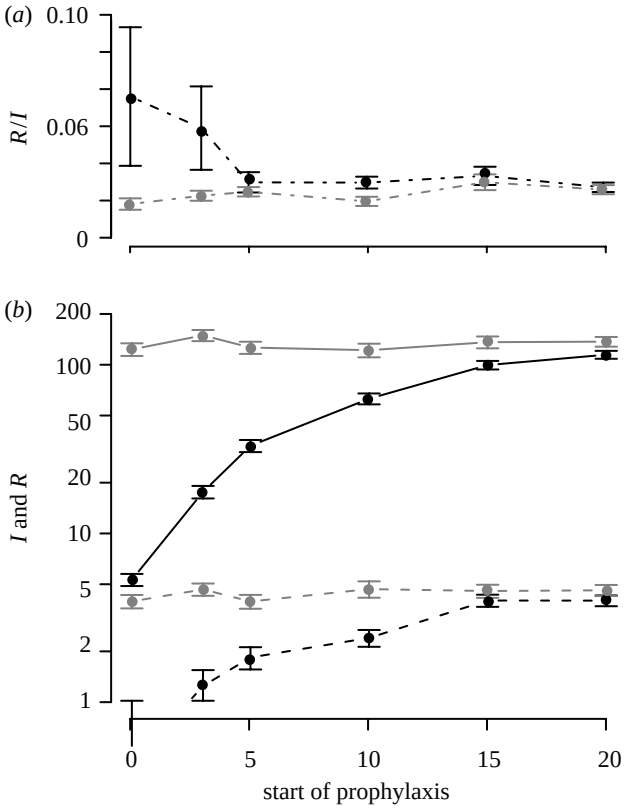

Figure 10. Impact of the timing of prophylaxis compared to treatment (*a*) on the proportion of resistance and (*b*) on the total number of infected and resistant cases. The dots represent the mean value of simulations having generated at least one secondary case, among 100 simulations. Error bars represent standard errors. There are four subpopulations, the total size of the population is $N=500$ and migration $=10^{-3}$. Grey, treatment; black, prophylaxis. Solid line, infected cases; dashed line, resistant cases; dot-dashed line, proportion of resistant cases among the infected; mean $\pm$ s.e.

population are unrealistic. However, the main aim of our paper was to study the effect of population fragmentation in isolation, rather than predict the level of resistance for a realistically structured population. To this end, we extended one of the simplest published influenza models (Stilianakis *et al.* 1998) into one which allowed for varying degrees of population fragmentation. This conceptual study has its justification because it allows us to extrapolate the predictions of simple models—assuming homogeneously mixed host populations and deterministic dynamics—to situations in which spatial population structure and stochasticity are important. To make this model more realistic, one could analyse more realistic network topologies and population structures. Additionally, one could also include aspects of the within-host dynamics of influenza infection and age structure, in particular because some key parameters of influenza epidemics vary with age (Ferguson *et al.* 2003; Doherty *et al.* 2006).

In spite of the lack of realism of the population structure in our model, our conclusions are similar to the ones made using very detailed models of pandemic influenza. Ferguson *et al.* (2005, 2006), Longini *et al.* (2005) and Germann *et al.* (2006) show that targeted antiviral prophylaxis is the best medical intervention, and that if R_0 is high, a combination of medical and non-medical interventions (such as social distancing) have to be adopted to mitigate the pandemic. Considering social distancing as a measure that increases population fragmentation, we show that prophylaxis is the best intervention and that its effects are increased by population fragmentation (figures 5 and 9). Lipsitch *et al.* (2007) also studied the emergence of resistance, albeit without incorporating any spatial structure of the population. One of their key results is that resistance levels are higher when non-drug interventions are adopted. Hereby, they modelled non-drug interventions by simply reducing the basic reproduction number R_0 of the pandemic strain. In our model, we can model non-drug interventions, such as social distancing or quarantine, by increasing the population fragmentation. In a more fragmented population, similar to Lipsitch *et al.* (2007), we observe that the prevalence of resistance is reduced, while the proportion of resistance increases (figure 11). This is due to the fact that in a fragmented population the epidemic spreads slower and prophylaxis hits the epidemic during an earlier state (figure 5*c–e*).

Only few studies on the containment or mitigation of an influenza pandemic investigate the emergence of resistant viruses, but most authors acknowledge the challenge that the emergence of resistant viruses represents (Ferguson *et al.* 2005, 2006; Germann *et al.* 2006). We hope that the potential emergence of drug resistance will be incorporated into more mathematical studies (especially the very detailed ones) so that we can face up to this challenge.

APPENDIX A. DETERMINISTIC MODEL: EQUATIONS

A.1. Dynamics without drugs

Without any public health intervention, the course of the disease is modelled by using an SII_SR model, which has been extended to a metapopulation

$\forall i \in \{1, \ldots, n\}$,

$$\begin{cases} \dot{S}_i = -(\beta_{1,i} I_i + \beta_{2,i} I_{s,i}) \cdot S_i + \mathcal{M}(S_i), \\ \dot{I}_i = (\beta_{1,i} I_i + \beta_{2,i} I_{s,i}) \cdot S_i - (\delta_1 + \gamma_1) \cdot I_i + \mathcal{M}(I_i), \\ \dot{I}_{s,i} = \delta_1 \cdot I_i - \gamma_2 \cdot I_{s,i} + \mathcal{M}(I_{s,i}), \end{cases} \tag{A 1}$$

where for each class C, $\dot{C} = \mathrm{d}C/\mathrm{d}t$ and C_i refers to the number of individuals of this class present in subpopulation i, $1 \leq i \leq n$. Refer to table 2 for the description of the variables and table 3 for the values of the parameters. As defined in the main text, the migration parameter $\mathcal{M}$ is

$$\mathcal{M}(C_i) = -\sum_{j=1}^{n} \mu_{i,j} \cdot C_i + \sum_{j=1}^{n} (\mu_{j,i} \cdot C_j). \tag{A 2}$$

The total number of individuals in the population, N, is constant, because no demographic process is considered. Then, always, $S+I+I_S+R=N$. This is the reason why the equations for the recovered class R are not written here.

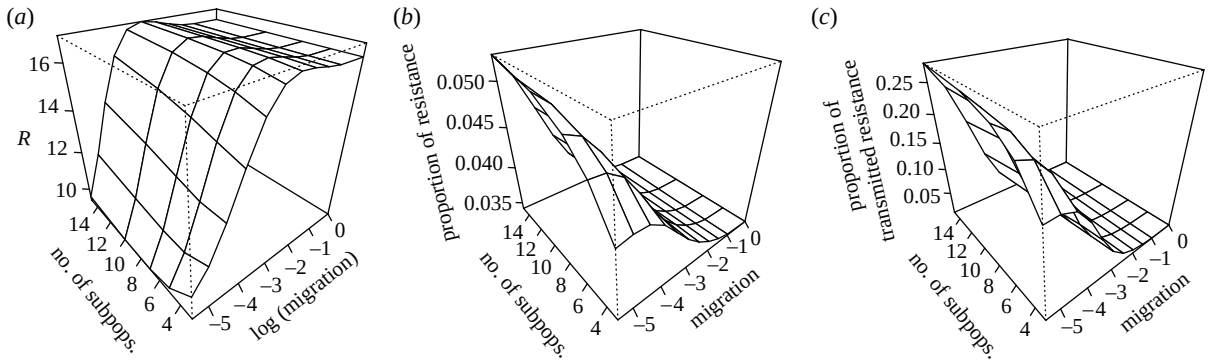

Figure 11. Impact of population fragmentation on the emergence of resistance, when prophylaxis is performed. Prophylaxis starts on day 5, island structure. $N=500$.(*a*) Effect on the total number of resistant cases. (*b*) Effect on the proportion of resistant cases among total infected cases. (*c*) Effect on the proportion of resistant cases due to transmission of the resistant strain, among total resistant cases.

Table 2. Variables of the models.

variable	no. of …individuals
S	susceptible
S_{pr}	susceptible, receiving chemoprophylaxis
I	infected, untreated, asymptomatic
I_{s}	infected, untreated, symptomatic
I_{r}	infected, untreated, asymptomatic, shedding resistant virus
$I_{\mathrm{s,r}}$	infected, untreated, symptomatic, shedding resistant virus
I_{tr}	infected, treated, asymptomatic
$I_{\mathrm{s,tr}}$	infected, treated, symptomatic
$I_{\mathrm{r,tr}}$	infected, treated, asymptomatic, shedding resistant virus
$I_{\mathrm{s,r,tr}}$	infected, treated, symptomatic, shedding resistant virus

Table 3. Parameters of the models. (Refer to Regoes & Bonhoeffer (2006) for justification of the chosen values, as well as Stilianakis *et al.* (1998).)

parameter	description	value
β_1	transmission rate between I and S	} scaled such that $R_0^{\mathrm{s}}=4.5$
β_2	transmission rate between I_{s} and S	
$\beta_{1,\mathrm{r}}$	transmission rate between I_{r} and S	} scaled such that $R_0^{\mathrm{r}}=0.45$
$\beta_{2,\mathrm{r}}$	transmission rate between $I_{\mathrm{s,r}}$ and S	
$K_{2,1}$	relative infectivity of I_{s} and $I_{\mathrm{s,r}}$ (compared to I and I_{r} respectively)	10
p_1	relative infectivity of I_{tr} (compared to I)	0.67
p_2	relative infectivity of $I_{\mathrm{s,tr}}$ (compared to I_{s})	0.67
p_3	relative susceptibility of S_{pr} to infection with I (compared to S)	0.5
p_4	relative susceptibility of S_{pr} to infection with I_{s} (compared to S)	0.5
p_5	relative susceptibility of S_{pr} to infection with I_{tr} (compared to S)	0.5×0.67
p_6	relative susceptibility of S_{pr} to infection with $I_{\mathrm{s,tr}}$ (compared to S)	0.5×0.67
δ_1	rate of development of symptoms by I	$0.5\ \mathrm{d}^{-1}$
δ_2	rate of development of symptoms by I_{r}	$0.5\ \mathrm{d}^{-1}$
δ_3	rate of development of symptoms by I_{tr}	$0.1\ \mathrm{d}^{-1}$
δ_4	rate of development of symptoms by $I_{\mathrm{r,tr}}$	$0.5\ \mathrm{d}^{-1}$
θ_1	rate of chemoprophylaxis of S	$0\ \mathrm{d}^{-1}$
θ_2	rate of chemoprophylaxis of I and I_{r}	$0\ \mathrm{d}^{-1}$
θ_3	rate of treatment of I_{s} and $I_{\mathrm{s,r}}$	$0.7\ \mathrm{d}^{-1}$
γ_1	recovery rate from asymptomatic infection	$0.5\ \mathrm{d}^{-1}$
γ_2	recovery rate from symptomatic infection	$0.25\ \mathrm{d}^{-1}$
r_1	relative recovery of I_{tr} compared to I	2
r_2	relative recovery of $I_{\mathrm{s,tr}}$ compared to I_{s}	1.5
$q_1\kappa$	rate of acquired drug resistance in I_{tr}	$0.036\ \mathrm{d}^{-1}$
$q_2\kappa$	rate of acquired drug resistance in $I_{\mathrm{s,tr}}$	$0.036\ \mathrm{d}^{-1}$

A.2. Dynamics with intervention

When treatment or prophylaxis is performed, the equations describing the course of the disease are the following:

$$
\begin{aligned}
&\forall i \in \{1,\ldots,n\},\\
&\dot{S}_i = -(\beta_{1,i} I_i + \beta_{2,i} I_{\mathrm{s},i} + \beta_{1,\mathrm{r},i} I_{\mathrm{r},i} + \beta_{2,\mathrm{r},i} I_{\mathrm{s,r},i} + p_1\beta_{1,i} I_{\mathrm{tr},i}\\
&\quad + p_2\beta_{2,i} I_{\mathrm{s,tr},i} + \beta_{1,\mathrm{r},i} I_{\mathrm{r,tr},i} + \beta_{2,\mathrm{r},i} I_{\mathrm{s,r,tr},i}) S_i\\
&\quad - \theta_1 S_i + \mathcal{M}(S_i)\\
&\dot{S}_{\mathrm{pr},i} = -(p_3\beta_{1,i} I_i + p_4\beta_{2,i} I_{\mathrm{s},i} + \beta_{1,\mathrm{r},i} I_{\mathrm{r},i} + \beta_{2,\mathrm{r},i} I_{\mathrm{s,r},i}\\
&\quad + p_5\beta_{1,i} I_{\mathrm{tr},i} + p_6\beta_{2,i} I_{\mathrm{s,tr},i} + \beta_{1,\mathrm{r},i} I_{\mathrm{r,tr},i} + \beta_{2,\mathrm{r},i} I_{\mathrm{s,r,tr},i})\\
&\quad \times S_{\mathrm{pr},i} + \theta_1 S_i + \mathcal{M}(S_{\mathrm{pr},i})\\
&\dot{I}_i = (\beta_{1,i} I_i + \beta_{2,i} I_{\mathrm{s},i} + p_1\beta_{1,i} I_{\mathrm{tr},i} + p_2\beta_{2,i} I_{\mathrm{s,tr},i}) S_i\\
&\quad - (\gamma_1 + \delta_1 + \theta_2) I_i + \mathcal{M}(I_i)\\
&\dot{I}_{\mathrm{s},i} = \delta_1 I_i - (\gamma_2 + \theta_3) I_{\mathrm{s},i} + \mathcal{M}(I_{\mathrm{s},i})\\
&\dot{I}_{\mathrm{r},i} = (\beta_{1,\mathrm{r},i} I_{\mathrm{r},i} + \beta_{2,\mathrm{r},i} I_{\mathrm{s,r},i} + \beta_{1,\mathrm{r},i} I_{\mathrm{r,tr},i} + \beta_{2,\mathrm{r},i} I_{\mathrm{s,r,tr},i}) S_i\\
&\quad - (\gamma_1 + \delta_2 + \theta_2) I_{\mathrm{r},i} + \mathcal{M}(I_{\mathrm{r},i})\\
&\dot{I}_{\mathrm{s,r},i} = \delta_2 I_{\mathrm{r},i} - (\gamma_2 + \theta_3) I_{\mathrm{s,r},i} + \mathcal{M}(I_{\mathrm{s,r},i})\\
&\dot{I}_{\mathrm{tr},i} = (p_3\beta_{1,i} I_i + p_4\beta_{2,i} I_{\mathrm{s},i} + p_5\beta_{1,i} I_{\mathrm{tr},i} + p_6\beta_{2,i} I_{\mathrm{s,tr},i}) S_{\mathrm{pr},i}\\
&\quad - (r_1\gamma_1 + \delta_3 + q_1\kappa) I_{\mathrm{tr},i} + \theta_2 I_i + \mathcal{M}(I_{\mathrm{tr},i})\\
&\dot{I}_{\mathrm{s,tr},i} = \delta_3 I_{\mathrm{tr},i} - (r_2\gamma_2 + q_2\kappa) I_{\mathrm{s,tr},i} + \theta_3 I_{\mathrm{s},i} + \mathcal{M}(I_{\mathrm{s,tr},i})\\
&\dot{I}_{\mathrm{r,tr},i} = (\beta_{1,\mathrm{r},i} I_{\mathrm{r},i} + \beta_{2,\mathrm{r},i} I_{\mathrm{s,r},i} + \beta_{1,\mathrm{r},i} I_{\mathrm{r,tr},i} + \beta_{2,\mathrm{r},i} I_{\mathrm{s,r,tr},i}) S_{\mathrm{pr},i}\\
&\quad - (\gamma_1 + \delta_4) I_{\mathrm{r,tr},i} + q_1\kappa I_{\mathrm{tr},i} + \theta_2 I_{\mathrm{r},i} + \mathcal{M}(I_{\mathrm{r,tr},i})\\
&\dot{I}_{\mathrm{s,r,tr},i} = \delta_4 I_{\mathrm{r,tr},i} - \gamma_2 I_{\mathrm{s,r,tr},i} + q_2\kappa I_{\mathrm{s,tr},i} + \theta_3 I_{\mathrm{s,r},i} + \mathcal{M}(I_{\mathrm{s,r,tr},i}).
\end{aligned}
\tag{A 3}
$$

A.3. Total numbers of infected and resistant cases

We calculate the total number of infected cases generated during the epidemic

$$
\mathcal{I} = S_0 - \sum_{i=1}^{n} \left(S_i(t_{\mathrm{end}}) + S_{\mathrm{pr},i}(t_{\mathrm{end}})\right), \tag{A 4}
$$

where $S_0 = \sum_{i=1}^{n} S_i(0) + S_{\mathrm{pr},i}(0)$.

We also determine the total number of individuals having shed resistant viruses during the epidemic (i.e. total number of resistant cases)

$$
\mathcal{R} = \mathcal{R}_{\mathrm{transmitted}} + \mathcal{R}_{\mathrm{de\ novo}}, \tag{A 5}
$$

where

$$
\begin{aligned}
\mathcal{R}_{\mathrm{transmitted}} = \int_0^{t_{\mathrm{end}}} \sum_{i=1}^{n} [&(\beta_{1,\mathrm{r},i} I_{\mathrm{r},i} + \beta_{2,\mathrm{r},i} I_{\mathrm{s,r},i} + \beta_{1,\mathrm{r},i} I_{\mathrm{r,tr},i}\\
&+ \beta_{2,\mathrm{r},i} I_{\mathrm{s,r,tr},i})(S_i + S_{\mathrm{pr},i})]\,\mathrm{d}t,
\end{aligned}
\tag{A 6}
$$

$$
\mathcal{R}_{\mathrm{de\ novo}} = \int_0^{t_{\mathrm{end}}} \sum_{i=1}^{n} [q_1\kappa I_{\mathrm{tr},i} + q_2\kappa I_{\mathrm{s,tr},i}]\,\mathrm{d}t. \tag{A 7}
$$

The proportion of resistance is $\mathcal{R}/\mathcal{I}$, and the proportion of de novo resistance is $\mathcal{R}_{\mathrm{de\ novo}}/\mathcal{R}$.

APPENDIX B. CALCULATION OF THE BASIC REPRODUCTIVE NUMBERS

To calculate the basic reproductive numbers of the sensitive and resistant strains in our deterministic models of influenza epidemics we used the so-called next-generation method described by Heffernan *et al.* (2005). Since the basic reproductive numbers depend on the intervention, we deal with the three interventions separately.

B.1. R_0 without intervention

The I and I_{S} classes are *infected* classes. The disease-free equilibrium corresponds to $X_0 = \{S_0, 0, 0\}$. Given the equations of the model (A 1),

$$
F = \begin{pmatrix} \beta_1 S_0 & \beta_2 S_0 \\ 0 & 0 \end{pmatrix} \quad \text{and} \quad V = \begin{pmatrix} \delta_1 + \gamma_1 & 0 \\ -\delta_1 & \gamma_2 \end{pmatrix}.
$$

V is invertible, because it is triangular, and

$$
FV^{-1} = \begin{pmatrix} \dfrac{\beta_1 S_0}{\delta_1 + \gamma_1} + \dfrac{\beta_2 \delta_1 S_0}{\gamma_2(\delta_1 + \gamma_1)} & \dfrac{\beta_2 S_0}{\gamma_2} \\ 0 & 0 \end{pmatrix}.
$$

The characteristic equation associated to FV^{-1} is

$$
P(\lambda) = \lambda \cdot \left[\lambda - \left(S_0 \cdot \frac{\beta_1 + \frac{\beta_2\delta_1}{\gamma_2}}{\delta_1 + \gamma_1}\right)\right],
$$

and hence the basic reproductive number R_0 has the form

$$
R_0 = S_0 \cdot \left(\beta_1 + \frac{\beta_2\delta_1}{\gamma_2}\right) \cdot \frac{1}{\delta_1 + \gamma_1}. \tag{B 1}
$$

Note that this formula can be obtained in a more straightforward way: the stable state approximation at the disease-free equilibrium can be used to simplify the system. With $X^* = \{S^*, I^*, I_s^*\} = \{S_0, 0, 0\}$,

$$
\dot{I}_{\mathrm{s}} = 0 \Rightarrow I_{\mathrm{s}}^* = \frac{\delta_1}{\gamma_2} \cdot I^*.
$$

Then,

$$
\dot{I} > 0 \Leftrightarrow S_0 \cdot \left(\beta_1 + \frac{\beta_2\delta_1}{\gamma_2}\right) \cdot \frac{1}{\delta_1 + \gamma_1} > 0,
$$

which leads to the same formula for R_0 as previously.

B.1.1. Consequence: R_0 and the βs. In the metapopulation model, we scale the βs in order to keep the same R_0 in all the subpopulations, irrespective of their size. With $K_{2,1} = \beta_2/\beta_1$, according to (A 8),

$$
\beta_1 = \frac{R_0(\delta_1 + \gamma_1)}{S_0(1 + K_{2,1}\delta_1/\gamma_2)} \propto \frac{R_0}{S_0}. \tag{B 2}
$$

Scaling the βs amounts to writing the ODEs in the form $\mathrm{d}I/\mathrm{d}t = -\beta SI/N\ldots$ (frequency-dependant versus density-dependant previously).

B.2. R_0 in a treated population

In the full model (A 3), two different strains, the drug-sensitive one and the drug-resistant one, have to be considered. Castillo-Chavez *et al.* (2002) show how to extend the next generation method to a model with

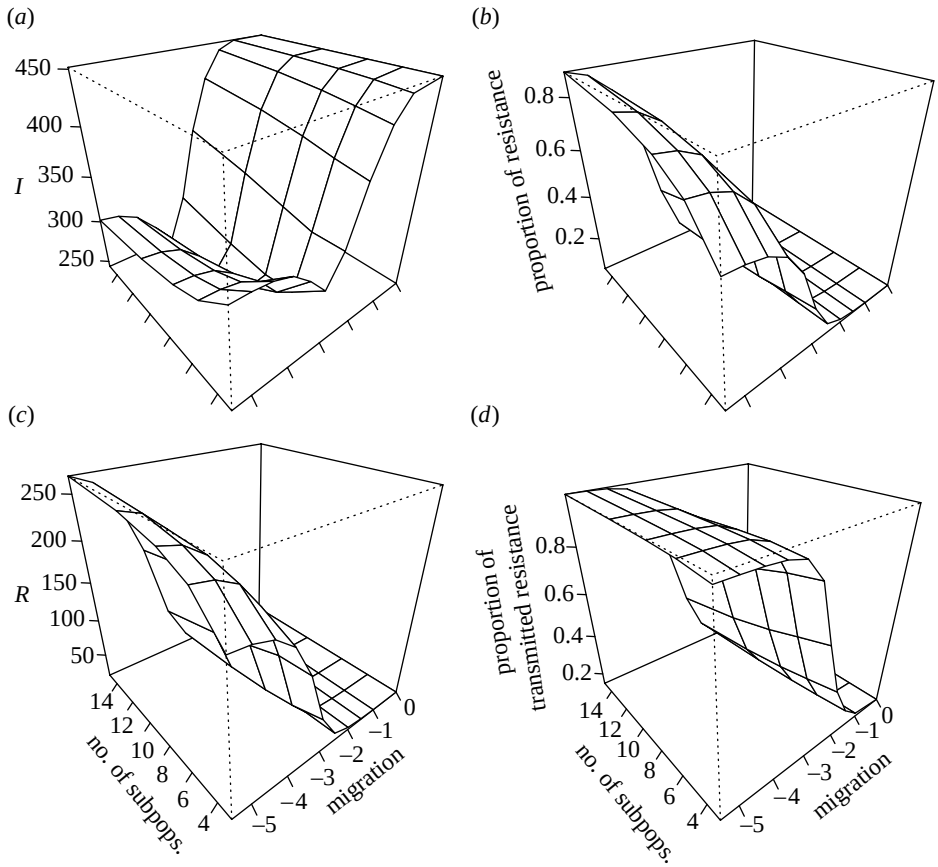

Figure 12. Impact of population fragmentation on the emergence of resistance, when prophylaxis is performed and when $R_0^{\mathrm{r}} = 1.5$. Prophylaxis starts on day 5, island structure. $N=500$. (*a*) Effect on the total number of infected cases. (*b*) Effect on the total number of resistant cases. (*c*) Effect on the proportion of resistant cases among total infected cases. (*d*) Effect on the proportion of resistant cases due to transmission of the resistant strain, among total resistant cases.

different strains. The same results are obtained when the method is applied to the full model, or when it is only applied to relevant equations. For the sake of brevity, only this second method is shown here.

The relevant classes here are $S,I,I_{\mathrm{s}},I_{\mathrm{r}},I_{\mathrm{s,r}},I_{\mathrm{s,tr}},I_{\mathrm{s,r,tr}}$, because treatment is only given to symptomatically infected people. The disease-free equilibrium is $X_0=\{S_0, 0, 0, 0, 0\}$.

Applying the next generation method to the *infected* compartment, the following matrices are obtained:

$$F = \begin{pmatrix} \beta_1 S_0 & \beta_2 S_0 & 0 & 0 & p_2\beta_2 S_0 & 0 \\ 0 & 0 & 0 & 0 & 0 & 0 \\ 0 & 0 & \beta_{1\mathrm{r}} S_0 & \beta_{2\mathrm{r}} S_0 & 0 & \beta_{2\mathrm{r}} S_0 \\ 0 & 0 & 0 & 0 & 0 & 0 \\ 0 & 0 & 0 & 0 & 0 & 0 \\ 0 & 0 & 0 & 0 & 0 & 0 \end{pmatrix},$$

$$V = \begin{pmatrix} \gamma_1+\delta_1+\theta_2 & 0 & 0 & 0 & 0 & 0 \\ -\delta_1 & \gamma_2+\theta_3 & 0 & 0 & 0 & 0 \\ 0 & 0 & \gamma_1+\delta_2+\theta_2 & 0 & 0 & 0 \\ 0 & 0 & -\delta_2 & \gamma_2+\theta_3 & 0 & 0 \\ 0 & -\theta_3 & 0 & 0 & r_2\gamma_2+q_2\kappa & 0 \\ 0 & 0 & 0 & -\theta_3 & -q_2\kappa & \gamma_2 \end{pmatrix}.$$

After having determined the non-null eigenvalues of FV^{-1}, we obtain, with $\theta_1=\theta_2=0$,

$$R_0^{\mathrm{r}} = S_0 \cdot \left(\beta_{1\mathrm{r}} + \frac{\beta_{2\mathrm{r}}\delta_2}{\gamma_2}\right) \cdot \frac{1}{\delta_2+\gamma_1}$$

and

$$R_0^{\mathrm{s}} = S_0 \cdot \left(\beta_1 + \frac{\beta_2\delta_1}{\gamma_2+\theta_3} + \frac{p_2\beta_2\delta_1\theta_3}{(\gamma_2+\theta_3)(q_2\kappa+r_2\gamma_2)}\right) \cdot \frac{1}{\delta_1+\gamma_1}. \tag{B3}$$

With our range of parameters, $R_0^{\mathrm{sensitive}} < R_0$. Treatment indeed lowers the infectivity.

B.3. $\mathbf{R_0}$ in a prophylaxed population

The relevant classes here are $S_{\mathrm{pr}},I_{\mathrm{tr}},I_{\mathrm{s,tr}},I_{\mathrm{r,tr}},I_{\mathrm{s,r,tr}}$, because everybody in the population gets either treatment (if symptomatically infected) or prophylaxis (otherwise). The disease-free equilibrium is $X_0=\{S_0, 0, 0, 0, 0\}$.

The following matrices are obtained:

$$F = \begin{pmatrix} p_5\beta_1 S_0 & p_6\beta_2 S_0 & 0 & 0 \\ 0 & 0 & 0 & 0 \\ 0 & 0 & \beta_{1\mathrm{r}} S_0 & \beta_{2\mathrm{r}} S_0 \\ 0 & 0 & 0 & 0 \end{pmatrix},$$

$$V = \begin{pmatrix} r_1\gamma_1 + \delta_3 + q_1\kappa & 0 & 0 & 0 \\ -\delta_3 & r_2\gamma_2 + q_2\kappa & 0 & 0 \\ -q_1\kappa & 0 & \gamma_1 + \delta_4 & 0 \\ 0 & -q_2\kappa & -\delta_4 & \gamma_2 \end{pmatrix}.$$

After having determined the non-null eigenvalues of FV^{-1}, we obtain, with $\theta_1 = \theta_2 = 0$,

$$R_0^{\mathrm{r}} = S_0 \cdot \left(\beta_{1\mathrm{r}} + \frac{\beta_{2\mathrm{r}}\delta_4}{\gamma_2} \right) \cdot \frac{1}{\delta_4 + \gamma_1}$$

and

$$R_0^{\mathrm{s}} = S_0 \cdot \left(p_5\beta_1 + \frac{p_6\beta_2\delta_3}{q_2\kappa + r_2\gamma} \right) \cdot \frac{1}{r_1\gamma_1 + q_1\kappa + \delta_3}. \quad \text{(B 4)}$$

B.4. R_0 in the metapopulation

The next generation method yields the same results in a metapopulation as in a single population (provided that the βs are scaled, equation (A 9)). Calculations are done with an island-shape metapopulation, where all subpopulations have the same size. Moreover, an epidemic generates the same number of infections in a metapopulation as in a single population of the same total size (figure 4 in the main text), which confirms our result.

APPENDIX C. RELAXING SOME PARAMETERS

C.1. Deterministic simulations with a higher R_0^{r}

In the main text of our article, we assumed a high fitness cost of the resistant strain and set $R_0^{\mathrm{r}} = 0.45 = R_0^{\mathrm{s}}/10$. This value may be too low to describe resistant strain during a pandemic because compensatory mutations could restore the fitness of the resistant virus.

To assess the robustness of our results with regard to our choice of R_0^{r} we conducted a simulation with higher values of R_0^{r}. Figure 12 shows simulations performed with $R_0^{\mathrm{r}} = 1.5$. The simulations in this figure are done with exactly the same parameters as figure 11, except that $R_0^{\mathrm{r}} = 1.5$.

For $R_0^{\mathrm{r}} = 1.5$, we obtain similar prevalences and levels of resistance as for $R_0^{\mathrm{r}} = 0.45$ (compare figure 12*b–d* with figure 11*a–c*). The values are higher in figure 12 because R_0^{r} is higher and above 1 (the resistant strain can sustain an epidemic by itself now).

The results for the total number of infections (figure 12*a*) differ. The prevalence increases when the population is highly fragmented. This is due to the fact that the resistant strain with $R_0^{\mathrm{r}} = 1.5$ cannot be controlled by prophylaxis anymore, and in fragmented populations prophylaxis hits the epidemic during an earlier stage. In a fragmented population, therefore, more susceptible hosts remain to be infected by the resistant strain.

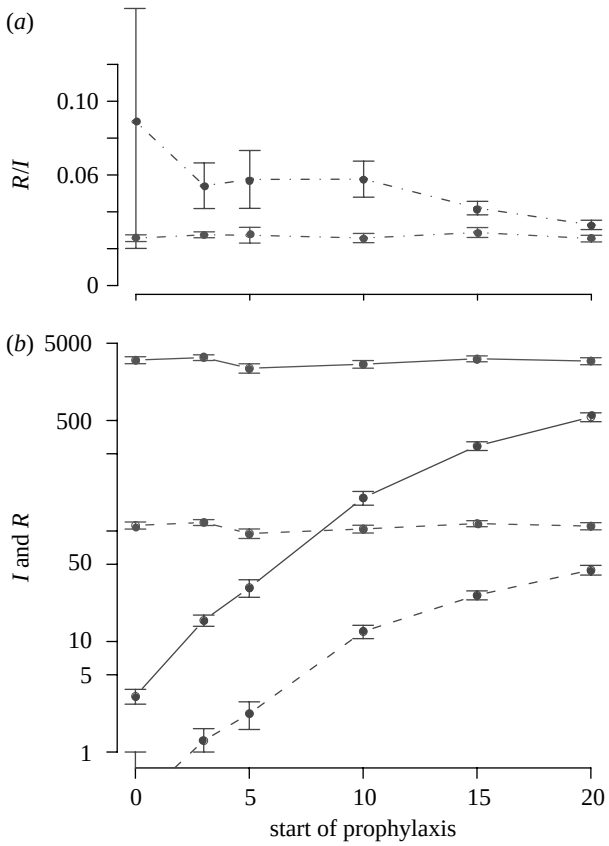

Figure 13. Same figure as figure 10, but with a total population size $N = 5000$. Impact of the timing of prophylaxis compared to treatment (*a*) on the proportion of resistance and (*b*) on the total number of infected and resistant cases. The dots represent the mean value of simulations having generated at least one secondary case, among 100 simulations. Error bars represent standard errors. There are four subpopulations, the total size of the population is $N = 5000$ and migration $= 10^{-3}$. Grey, treatment; black, prophylaxis. Solid line, infected cases; dashed line, resistant cases; dot-dashed line, proportion of resistant cases among the infected; mean $\pm$ s.e.

C.2. Stochastic simulations with a greater population size

We also investigated the impact of larger population sizes on our stochastic simulations. In figure 13 we used the same parameters as in figure 10, except that we set the total population size $N = 5000$ instead of $N = 500$ as in the main text. For $N = 5000$, we obtain similar results to those with $N = 500$: as expected, the total number of infected (I) and resistant (R) hosts is higher, but the prevalences (I/R and R/N) are the same. The proportion of resistance and the impact of proph.start are also similar.

REFERENCES

Anderson, R. M. & May, R. M. 1991 *Infectious diseases of humans*. Oxford, UK: Oxford University Press.

Bright, R., Shay, D., Shu, B., Cox, N. & Klimov, A. 2006 Adamantane resistance among influenza a viruses isolated early during the 2005–2006 influenza season in the United States. *JAMA* **295**, 891–894. (doi:10.1001/jama.295.8.joc60020)

Castillo-Chavez, C., Feng, Z. & Huang, W. 2002 On the computation R0 and its role on global stability. In *Mathematical approaches for emerging and reemerging infectious diseases: an introduction* (eds C. Castillo-Chavez, P. van den Driessche, D. Kirschner & A.-A. Yakubu), pp. 229–250. Reading, MA: Springer.

de Jong, M. D. *et al.* 2005 Brief report—Oseltamivir resistance during treatment of influenza A (H5N1) infection. *N. Engl. J. Med.* **353**, 2667–2672. (doi:10.1056/NEJMoa054512)

Diekmann, O., Heesterbeek, J. & Metz, J. 1990 On the definition and the computation of the basic reproduction ratio R0 in models for infectious-diseases in heterogeneous populations. *J. Math. Biol.* **28**, 365–382. (doi:10.1007/BF00178324)

Doherty, P. C., Turner, S. J., Webby, R. G. & Thomas, P. G. 2006 Influenza and the challenge for immunology. *Nat. Immunol.* **7**, 449–455. (doi:10.1038/ni1343)

Ferguson, N., Mallett, S., Jackson, H., Roberts, N. & Ward, P. 2003 A population-dynamic model for evaluating the potential spread of drug-resistant influenza virus infections during community-based use of antivirals. *J. Antimicrob. Chemother.* **51**, 977–990. (doi:10.1093/jac/dkg136)

Ferguson, N., Cummings, D., Cauchemez, S., Fraser, C., Riley, S., Meeyai, A., Iamsirithaworn, S. & Burke, D. 2005 Strategies for containing an emerging influenza pandemic in Southeast Asia. *Nature* **437**, 209–214. (doi:10.1038/nature04017)

Ferguson, N. M., Cummings, D. A. T., Fraser, C., Cajka, J. C., Cooley, P. C. & Burke, D. S. 2006 Strategies for mitigating an influenza pandemic. Nature advanced online publication. (doi:10.1038/nature04795)

Germann, T. C., Kadau, K., Longini, I. M. & Macken, C. A. 2006 Mitigation strategies for pandemic influenza in the United States. *Proc. Natl Acad. Sci. USA* **103**, 5935–5940. (doi:10.1073/pnas.0601266103)

Gillespie, D. 1976 General method for numerically simulating stochastic time evolution of coupled chemical-reactions. *J. Comput. Phys.* **22**, 403–434. (doi:10.1016/0021-9991(76)90041-3)

Grenfell, B. & Harwood, J. 1997 (Meta)population dynamics of infectious diseases. *Trends Ecol. Evol.* **12**, 395–399. (doi:10.1016/S0169-5347(97)01174-9)

Gubareva, L. V., Kaiser, L., Matrosovich, M. N., Soo-Hoo, Y. & Hayden, F. G. 2001 Selection of influenza virus mutants in experimentally infected volunteers treated with oseltamivir. *J. Infect. Dis.* **183**, 523–531. (doi:10.1086/318537)

Heffernan, J., Smith, R. & Wahl, L. 2005 Perspectives on the basic reproductive ratio. *J. R. Soc. Interface* **2**, 281–293. (doi:10.1098/rsif.2005.0042)

Herlocher, M. L., Carr, J., Ives, J., Elias, S., Truscon, R., Roberts, N. & Monto, A. S. 2002 Influenza virus carrying an r292k mutation in the neuraminidase gene is not transmitted in ferrets. *Antivir. Res.* **54**, 99–111. (doi:10.1016/S0166-3542(01)00214-5)

Herlocher, M. L., Truscon, R., Elias, S., Yen, H. L., Roberts, N. A., Ohmit, S. E. & Monto, A. S. 2004 Influenza viruses resistant to the antiviral drug oseltamivir: trans mission studies in ferrets. *J. Infect. Dis.* **190**, 1627–1630. (doi:10.1086/424572)

Hess, G. 1996 Disease in metapopulation models: implications for conservation. *Ecology* **77**, 1617–1632. (doi:10.2307/2265556)

Hess, G., Randolph, S., Arneberg, P., Chemini, C., Furlanello, C., Harwood, J., Roberts, M. & Swinton, J. 2002 *The ecology of wildlife diseases,* pp. 102–118. Oxford, UK: Oxford University Press.

Heymann, D. L. 2006 Resistance to anti-infective drugs and the threat to public health. *Cell* **124**, 671–675. (doi:10.1016/j.cell.2006.02.009)

Hufnagel, L., Brockmann, D. & Geisel, T. 2004 Forecast and control of epidemics in a globalized world. *Proc. Natl Acad. Sci. USA* **101**, 15 124–15 129. (doi:10.1073/pnas.0308344101)

Kermack, W. O. & McKendrick, A. G. 1927 A contribution to the mathematical theory of epidemics. *Proc. R. Soc. A* **115**, 700–721. (doi:10.1098/rspa.1927.0118)

Kiso, M., Mitamura, K., Sakai-Tagawa, Y., Shiraishi, K., Kawakami, C., Kimura, K., Hayden, F., Sugaya, N. & Kawaoka, Y. 2004 Resistant influenza A viruses in children treated with oseltarnivir: descriptive study. *Lancet* **364**, 759–765. (doi:10.1016/S0140-6736(04)16934-1)

Lipsitch, M., Cohen, T., Murray, M. & Levin, B. R. 2007 Antiviral resistance and the control of pandemic influenza. *PLoS Med.* **4**, e15. (doi:10.1371/journal.pmed.0040015)

Longini, I., Nizam, A., Xu, S., Ungchusak, K., Hanshaoworakul, W., Cummings, D. & Halloran, M. 2005 Containing pandemic influenza at the source. *Science* **309**, 1083–1087. (doi:10.1126/science.1115717)

Mills, C. E., Robins, J. M. & Lipsitch, M. 2004 Transmissibility of 1918 pandemic influenza. *Nature* **432**, 904–906. (doi:10.1038/nature03063)

Moscona, A. 2005 Dec Oseltamivir resistance—disabling our influenza defenses. *N. Engl. J. Med.* **353**, 2633–2636. (doi:10.1056/NEJMp058291)

R Development Core Team, 2005. R: a language and environment for statistical computing. R Foundation for Statistical Computing, Vienna, Austria. See http://www.R-project.org.

Regoes, R. & Bonhoeffer, S. 2006 Emergence of drug-resistant influenza virus: population dynamical considerations. *Science* **312**, 389–391. (doi:10.1126/science.1122947)

Setzer, R. W. 2005 Odesolve: solvers for ordinary differential equations. R package version 0.5–13.

Smith, D. J. 2003 Applications of bioinformatics and computational biology to influenza surveillance and vaccine strain selection. *Vaccine* **21**, 1758–1761. (doi:10.1016/S0264-410X(03)00068-9)

Stilianakis, N. I., Perelson, A. S. & Hayden, F. G. 1998 Emergence of drug resistance during an influenza epidemic: insights from a mathematical model. *J. Infect. Dis.* **177**, 863–873.

Stiver, G. 2003 The treatment of influenza with antiviral drugs. *CMAJ* **168**, 49–57.

Webby, R. & Webster, R. 2003 Are we ready for pandemic influenza? *Science* **302**, 1519–1522. (doi:10.1126/science.1090350)

Yen, H. L., Herlocher, L. M., Hoffmann, E., Matrosovich, M. N., Monto, A. S., Webster, R. G. & Govorkova, E. A. 2005 Neuraminidase inhibitor-resistant influenza viruses may differ substantially in fitness and transmissibility. *Antimicrob. Agents Chemother.* **49**, 4075–4084. (doi:10.1128/AAC.49.10.4075-4084.2005)